Available online at www.sciencedirect.com

SciVerse ScienceDirect

Ceramics International 38 (2012) 5231–5237

CERAMICS
INTERNATIONAL

www.elsevier.com/locate/ceramint

High pressure synthesis of magnesium aluminate composites with $MoSi_2$ and Mo_5Si_3 in a self-sustaining manner

Z.I. Zaki [a,b,*], Nasser Y. Mostafa [a,c], M.M. Rashad [b]

[a] *Chemistry Department, Faculty of Science, Taif University, P.O. Box: 888 Al-Haweiah, Taif, Saudi Arabia*
[b] *Advanced Materials Division, Central Metallurgical R&D Institute (CMRDI), P.O. Box: 87 Helwan, Cairo, Egypt*
[c] *Chemistry Department, Faculty of Science, Suez Canal University, Ismailia 41522, Egypt*

Received 16 January 2012; received in revised form 3 March 2012; accepted 12 March 2012
Available online 20 March 2012

Abstract

Magnesium aluminate/$MoSi_2$ and magnesium aluminate/Mo_5Si_3 composites were successfully prepared by combustion synthesis with a special emphasis on the thermodynamic of the reactions involved in the process. The process involves loading of a very weak exothermic formation reaction of $MgAl_2O_4$ onto a highly exothermic formation reaction of $MoSi_2$ and Mo_5Si_3. The starting material was a blend of MoO_3, SiO_2, Al and MgO. The effect of Al grain size (−5 to −71 μm), MoO_3 stoichiometric value (0.7–1.25*x*), MgO additions (15–25 wt%) and working pressure (50 bar) on the synthesis process were investigated. Microstructure of the combustion products was inspected by SEM. It was found that using −5 μm grain size Al was necessary for reaction completion. Higher stoichiometric value of MoO_3 was found to be necessary to compensate for its volatilization from the reaction media. Addition of MgO as diluents reduced combustion temperature but unexpectedly it reacted with some amounts of SiO_2 and formed Mg_2SiO_2 phase and Mo_5Si_3 instead of $MoSi_2$. However, increasing the reaction pressure was found to be the most effective factor to suppress the MoO_3 volatilization. Thermodynamic study of the process revealed the production of entire phases in molten states whereas the adiabatic temperatures of the formation reaction of $MgAl_2O_4$/$MoSi_2$ and $MgAl_2O_4$/Mo_5Si_3 composites were 2408 and 3210 K, respectively.

Keywords: D. Silicides; $MoSi_2$; Mo_5Si_3; $MgAl_2O_4$; Combustion

1. Introduction

Magnesium aluminate spinel ($MgAl_2O_4$), an excellent refractory oxide, possesses useful physical, chemical and thermal properties, both at normal and elevated temperatures. It melts congruently at 2135 °C, shows high resistance to attack by most of the acids and alkalis and has low electrical losses. $MgAl_2O_4$ has mainly been used as refractory in heavy industry and as substrate for solid-state electronic devices. $MgAl_2O_4$ is widely used as sensing material to monitor humidity. Nowadays, new potential applications have been reported including: ceramic ultra-filtration membranes, electroinsulators, and optical materials [1–8]. Magnesium aluminate spinel was also used in the fields of environmental catalysis, petroleum processing and fine chemical production as a catalyst and a catalyst supporter [9,10]. $MoSi_2$ and its composites have received an increasing attention owing to their unique thermal, electrical and chemical properties and moderate density. Despite the weak mechanical properties and pest oxidation problems, $MoSi_2$ composites became important structural materials for application in oxidizing and aggressive environments specially as heating elements in high temperature furnaces [11]. To the best of our knowledge, designing of $MoSi_2$/$MgAl_2O_4$ and Mo_5Si_3/$MgAl_2O_4$ composites have not been discussed so far. These composites are expected to have electrical conductivity due to presence of Mo silicides while $MgAl_2O_4$ works as a matrix. Mo_5Si_3 has a more complex unit cell, which leads to better creep resistance. The creep rate of Mo_5Si_3 is lower than that of $MoSi_2$. Therefore, Mo_5Si_3 has been used as reinforcement for $MoSi_2$ and Si_3N_4 composites [12].

$MgAl_2O_4$ spinel and $MoSi_2$ ceramics have been prepared using various starting materials and preparation methods. Magnesia spinel was synthesized by co-precipitation [13,14],

---

[*] Corresponding author at: Chemistry Department, Faculty of Science, Taif University, P.O. Box: 888 Al-Haweiah, Taif, Saudi Arabia.
E-mail address: zakimohamed2000@yahoo.com (Z.I. Zaki).

0272-8842/$36.00
doi:10.1016/j.ceramint.2012.03.032

spray drying [15], freeze drying [16], and spray pyrolysis [17]. However, the common route for manufacturing magnesia spinel is the solid oxide reaction sintering. This process involves sintering of MgO and Al_2O_3 blends at 1600–1800 °C for several hours. A two-stage firing process was usually employed, a first one to complete the spinel formation and a second one to densify the formed spinel, which adversely affects the economy [18–20]. Other processes such as conventional arc-melting and casting, mechanical alloying, hot pressing, reaction sintering, plasma-spray processing, solid-state displacement reactions, and self-propagating high-temperature synthesis (SHS) have been used for synthesis of $MoSi_2$ [21–27].

Self-propagating high-temperature synthesis (SHS) is one of the rapidly growing cost-effective technologies used for synthesis of monolithic and composite in situ ceramics [25–27]. The principle of this technique is that the initial reagents, when ignited, spontaneously transform into products due to the exothermic heat of reaction. The advantages of SHS synthesis are very high-reaction rates and elimination of the need for high-temperature furnaces due to the immense energy release. Moreover, the SHS process represents a one-step manufacturing route capable of producing composites with homogeneous distribution of fine reinforcements. The major problem to be overcome in the SHS processing of refractory ceramics is the high-retained porosity of the synthesized products. Another difficulty associated with SHS process is the very high rates of reactions which makes controlling these reactions is not a simple process [26]. Another serious drawback of SHS is it's limitation to highly exothermic reaction.

In this work SHS was chosen to perform simultaneous synthesis of Mo–Si and magnesia spinel. Although $MoSi_2$ formation reaction is highly exothermic, spinel formation reaction is very weak exothermic reaction and cannot proceed alone in a self-sustaining manner. The factors affecting the combustion synthesis of $MoSi_2/MgAl_2O_4$ and $Mo_5Si_3/MgAl_2O_4$ composites were discussed. These included: effect of Al grain size, MoO_3 stoichiometric value, addition of MgO as diluents and working pressure. Thermodynamic of the different reactions involved in the process was also discussed.

2. Experimental

The materials used in this study were molybdenum trioxide of 99.5% purity and – 45 μm particle size (Atlantic Equipment Engineers, NJ, USA), aluminium metal powder of 99.5% purity and different grain sizes −71, −45, −36, and −5 μm (GFS Chemicals, Inc., USA) and −20 μm silica with 99% purity (Riedel-de Haen, Germany), MgO 99% purity and <5 μm particle size (BDH Chemicals Ltd., England).

The powders were mixed in the required molar ratio to form $MoSi_2/7/3MgAl_2O_4$ and $Mo_5Si_3/7MgAl_2O_4$ and dry blended in a slow rotating mill with alumina ball for 5 h. The powder mixture was uniaxially pressed without binder at 78 MPa into cylindrical compact of 20 mm height and 20 mm diameter to approximately 55% relative density.

The compact was transferred to combustion reactor and placed on a movable graphite plate. The reactor was evacuated and backfilled with pure argon at the required pressure. The ignition was carried out using a thin tungsten coil and ~1 mm above the compact. The electricity was supplied from an AC power source (30–40 A). In some cases the pressure inside the reactor vessel is increased to 50 bar argon. Detailed procedure of carrying out combustion reactions was provided elsewhere [26]. Different phases of the combustion products were identified by X-ray diffraction analysis using X-ray diffractometer (D8 Advanced Bruker AXS, GMbH, and Karlsruhe, Germany). Microstructure of specimens was investigated using Scanning Electron Microscope (SEM, Model JSM-5410, JEOL, Tokyo, Japan) equipped with electron dispersive spectroscopy (EDX). SEM investigation is conducted on fracture surfaces coated with gold to ensure good electrical conductivity of the entire components of the sample.

3. Results and discussion

3.1. Thermodynamic calculations

The combustion reaction between molybdenum trioxide, silica and aluminium blend powder is highly exothermic according to the equation:

$$MoO_3 + 2SiO_2 + 14/3Al = MoSi_2 + 7/3Al_2O_3 \qquad \Delta H = -1470\,\mathrm{kJ} \tag{1}$$

$$5MoO_3 + 3SiO_2 + 14Al = Mo_5Si_3 + 7Al_2O_3 \qquad \Delta H = -5561\,\mathrm{kJ} \tag{2}$$

On the other hand, the reaction between magnesia MgO and alumina to form magnesia spinel is very weak exothermic reaction in its nature and cannot proceed alone in a self-sustaining manner.

$$Al_2O_3 + MgO = MgAl_2O_4 \qquad \Delta H = -35.6\,\mathrm{kJ} \tag{3}$$

Addition of MgO to the reactant of reactions (1) and (2) in a stoichiometric amount equivalent to the quantity of liberated alumina generates the overall reactions (4) and (5).

$$MoO_3 + 2SiO_2 + 14/3Al + 7/3MgO = MoSi_2 + 7/3MgAl_2O_4 \tag{4}$$

$$5MoO_3 + 3SiO_2 + 14Al + 7MgO = Mo_5Si_3 + 7MgAl_2O_4 \tag{5}$$

Although reaction (3) cannot proceed alone in self-sustaining manner due to its very weak exothermic character, the overall reactions (4) and (5) is highly exothermic and the heat released by progress in reactions (1) and (2) can induce reaction (3) between the liberated alumina and the added magnesia. However for a reaction to progress in a self-sustaining manner, its adiabatic temperature should be equal to or higher than 1800 K as stated in the literatures [25]. Therefore calculating the adiabatic combustion temperature of reactions (4) and (5) is important for this study.

For reaction (4) the adiabatic combustion temperature and the fractions of molten phases of the products (if any) can be calculated from the following equation:

$$\begin{aligned}-\Delta H_{\mathrm{r},298} &+ \int_{298}^{T_o} C_\mathrm{p}(\mathrm{MoO_3} + 2\mathrm{SiO_2} + 14/3\mathrm{Al} + 7/3\mathrm{MgO})\mathrm{d}T \\ &= \int_{298}^{2303} C_\mathrm{p}(\mathrm{MoSi_2})_\mathrm{s}\mathrm{d}T + \int_{2303}^{T_\mathrm{ad}} C_\mathrm{p}(\mathrm{MoSi_2})_\mathrm{l}\mathrm{d}T + 7/3 \\ &\quad \times \int_{298}^{2408} C_\mathrm{p}(\mathrm{MgAl_2O_4})_\mathrm{s}\mathrm{d}T + 7/3 \\ &\quad \times \int_{2408}^{T_\mathrm{ad}} C_\mathrm{p}(\mathrm{MgAl_2O_4})_\mathrm{l}\mathrm{d}T + \alpha\Delta H_{\mathrm{f,MoSi_2}} \\ &\quad + 7/3\gamma\Delta H_{\mathrm{f,MgAl_2O_4}}\end{aligned} \tag{6}$$

And for reaction (5):

$$\begin{aligned}-\Delta H_{\mathrm{r},298} &+ \int_{298}^{T_o} C_\mathrm{p}(5\mathrm{MoO_3} + 3\mathrm{SiO_2} + 14\mathrm{Al} + 7\mathrm{SiO_2})\mathrm{d}T \\ &= \int_{298}^{2453} C_\mathrm{p}(\mathrm{Mo_5Si_3})_\mathrm{s}\mathrm{dT} + \int_{2453}^{T_\mathrm{ad}} C_\mathrm{p}(\mathrm{Mo_5Si_3})_\mathrm{l}\mathrm{d}T + 7 \\ &\quad \times \int_{298}^{2408} C_\mathrm{p}(\mathrm{MgAl_2O_4})_\mathrm{s}\mathrm{d}T + 7\int_{2408}^{T_\mathrm{ad}} C_\mathrm{p}(\mathrm{MgAl_2O_4})_\mathrm{l}\mathrm{d}T \\ &\quad + \alpha\Delta H_{\mathrm{f,Mo_5Si_3}} + 7\gamma\Delta H_{\mathrm{f,MgAl_2O_4}}\end{aligned} \tag{7}$$

where $\Delta H_{\mathrm{r},298}$ is the enthalpy change of reaction, C_p is the specific heat capacity, α and γ are the molten fractions; and ΔH_f is the enthalpy of fusion.

The adiabatic combustion temperature of reaction (4) at 298 K has a value of 2408 K which equal the melting point $MgAl_2O_4$ and greater than that of $MoSi_2$ (2303 K) as shown in Fig. 1. The calculation shows that at room temperature, the entire amounts of both $MoSi_2$ and 98 wt% of $MgAl_2O_4$ will be generated in the molten state and its corresponding phases will be crystalline from a molten state. Moreover, the value of adiabatic temperature of reaction (4) (2408 K) is higher than the empirical value (1800 K) which recommends the proceeding of the reaction in a self-sustaining manner [24]. Increasing the initial temperature of the reaction medium, away from 298 K, results in a linear increase in the corresponding adiabatic temperature. This behavior can be attributed to the consecutive accumulation of energy in the reactant materials.

A similar behavior is noticed with respect to reaction (5) as depicted in Fig. 2. The adiabatic temperature at room temperature is 3210 K which is higher than the melting points of both Mo_5Si_3 (2453 K) and that of $MgAl_2O_4$ (2408 K). This means that entire amounts of Mo_5Si_3 and $MgAl_2O_4$ will be produced in the molten phase. The very high temperature of the reaction at room temperature (3210 K) suggests that the reaction will be very vigorous. Increasing the initial temperature of the reaction medium, away from 298 K, results in a linear increase in the corresponding adiabatic temperature.

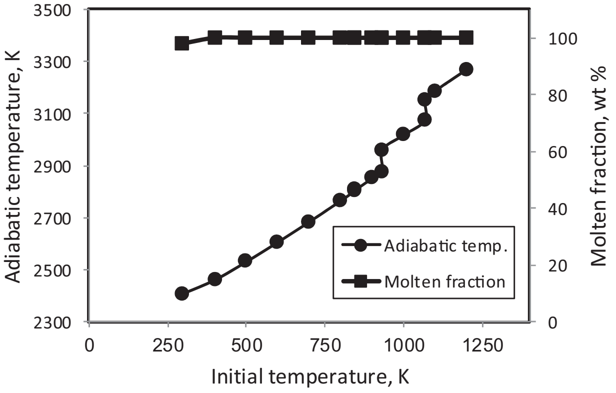

Fig. 1. Effect of initial temperature on the adiabatic temperature and molten fractions of $MoSi_2$ and $MgAl_2O_4$.

3.2. *Effect of aluminium metal grain size*

The effect of aluminium grain size on the ignition of the reaction (4) and the type of the obtained phases are discussed. The ignition of the samples is tried at room temperature for different Al grain sizes (−71, −45, −36 and −5 μm). The entire samples are successfully triggered at room temperature without the need of preheating step. This is due to the very high exothermic performance of reaction (4). Excess gases are noticed during the propagation of the combustion wave with the spreading of a white cloud inside the reactor. XRD patterns of the combustion products obtained from samples having different Al grain sizes are given in Fig. 3.

Generally, the figure shows the formation of magnesia spinel $MgAl_2O_4$ as the main phase and both $MoSi_2$ and its higher Mo-rich phase (Mo_5Si_3) match with moderate intensity lines. Free silicon Si is detected as a minor phase in entire samples. Reducing the aluminium grain size from −71 to −45 μm leads to a decreasing in the intensity of free silicon whereas finer

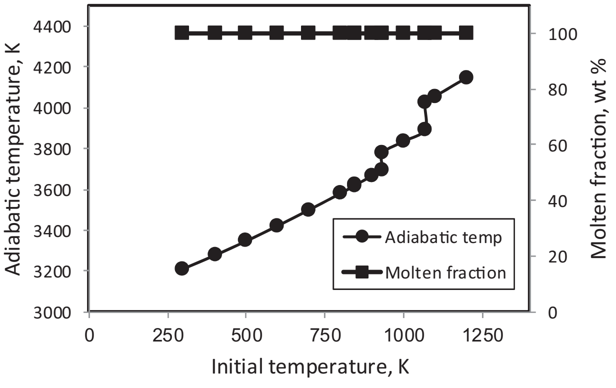

Fig. 2. Effect of initial temperature on the adiabatic temperature and molten fractions of Mo_5Si_3 and $MgAl_2O_4$.

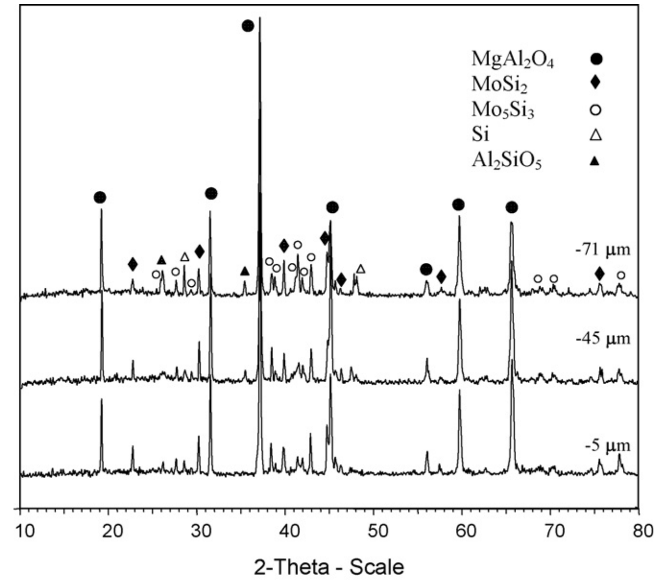

Fig. 3. XRD of combustion product prepared by using sample having different aluminium grain sizes.

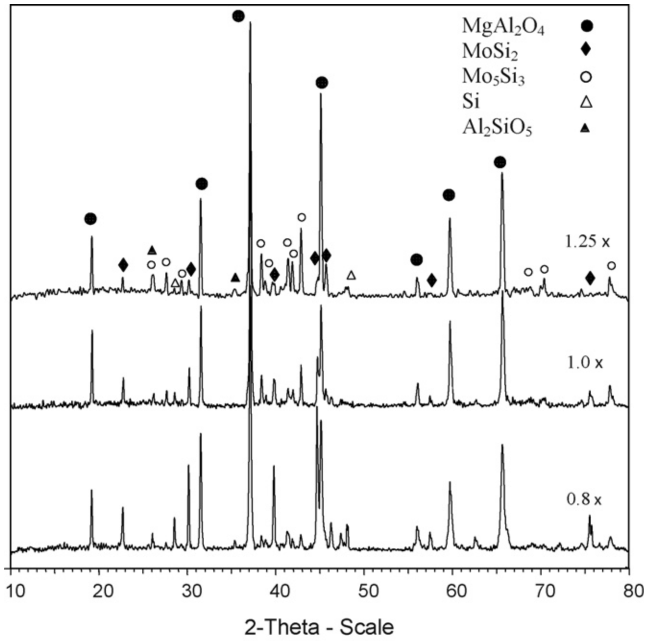

Fig. 4. Effect of MoO_3 stoichiometric value on the reaction completion.

aluminium grain sizes (−5 μm) has insignificant effect on free silicon. Furthermore, trace amounts of aluminium silicate Al_2SiO_5 are detected in case of −71 and −45 μm samples. The diffraction plane pattern of Al_2SiO_5 phase is completely disappears at −5 μm Al sample. These results ensure that the combustion reaction between MoO_3, SiO_2, MgO and Al powders successfully takes place with the production of target phases. However, the appearance of higher-rich molybdenum silicide Mo_5Si_3 phase and free silicon indicates some side reactions which may be avoided or minimized by optimizing the reaction conditions.

The presence of Mo_5Si_3 phase represents no problem to the expected application of the target composite ($MgAl_2O_4$/$MoSi_2$) because the grains of Mo_5Si_3 phase are considered to be reinforcement to $MoSi_2$ phase [12,28–31]. The co-existence of both Mo_5Si_3 and Si represents contradictory facts. The formation of Mo_5Si_3 phase indicates a deficiency of silicon and perfection of Mo while the presence of free silicon illustrates a deficiency of Mo and abundance of Si such that no chances for the formation of Mo-rich phase (Mo_5Si_3). It is worthy to mention that the formation of Mo_5Si_3 will also contribute to the appearance of free silicon because the Si content of Mo_5Si_3 is lower than that of $MoSi_2$. This behavior could be attributed to the volatilization of some amounts of MoO_3 (m.p. = 801 °C and b.p. = 1155 °C) before participating in the reaction during the approach of the combustion wave front as noticed by nicked eye (white cloud formation).

3.3. Effect of MoO_3 stoichiometric value

The stoichiometric amount of MoO_3 is investigated at 0.80 and 1.25 times the stoichiometric amount required for the formation of $MoSi_2$. Generally, increasing the amount of MoO_3 leads to more vigorous reaction with more densification of the white cloud. XRD profiles of these samples are given in Fig. 4. It is clear that increasing the MoO_3 stoichiometric value to 1.25 leads to the consumption of free silicon as indicated by the disappearance of the silicon phase from the diffraction pattern. A considerable increase in the intensity of Mo_5Si_3 phase with a parallel decrease in the intensity of the diffraction pattern of $MoSi_2$ phase is encountered. This is because the extra amounts of MoO_3 not only compensate for the volatilized amount but also contribute to more Mo in the reaction medium which increases the chance of Mo_5Si_3 formation.

On the other hand, decreasing the stoichiometric value of MoO_3 (0.8×) leads to increasing the amounts of both free silicon and $MoSi_2$ phase with a parallel decrease in the amount of Mo_5Si_3 as indicated in Fig. 4. This proves that the appearance of Si and Mo_5Si_3 at 1.0 stoichiometric value MoO_3 was due to the volatilization of some amounts of MoO_3 powder before its reaction.

3.4. Effect of MgO addition as dilution

In order to reduce the volatilized amounts of MoO_3 some amounts of MgO is added to the reaction mixture as inert phase. Addition of inert phase is thought to reduce the combustion temperature ($T_{ad} = 2408$ K) of the reaction by absorption of heat. The adiabatic temperature in case of MgO additions at room temperatures is calculated by introducing the term ''$x \int_{298}^{\mathrm{Tad}} C_p(\mathrm{MgO})_s \mathrm{dT}$'' to the right hand side of Eq. (6) and re-solving it to obtain T_{ad} where x is the amount of MgO in moles. Although, addition of 15 wt% of MgO absorbed ∼218 kJ to raise its temperature from room temperature to T_{ad}, the adiabatic temperature still constant at 2408 K where the percentage of $MgAl_2O_4$ melt is reduced from 98 wt% to 49.5 wt%. The amount of heat absorbed by MgO is calculated based on its heat capacity. On the other hand, 25 wt% additions

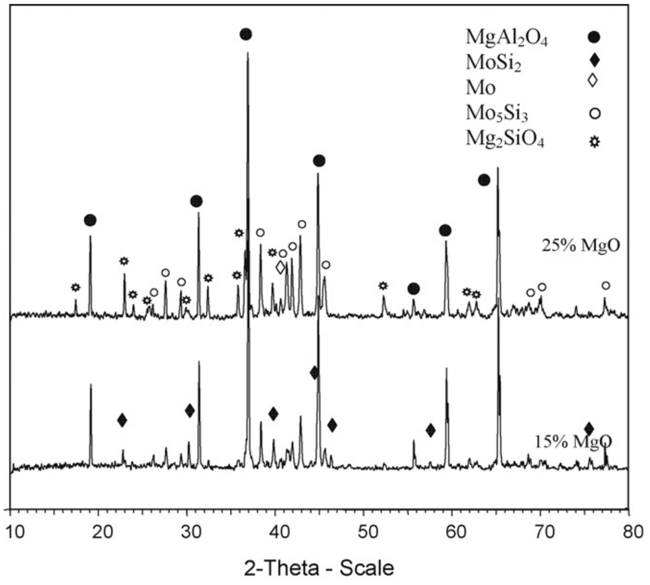

Fig. 5. Effect of MgO wt% on the combustion reaction of $gAl_2O_4/MoSi_2$.

of MgO absorbed 412 kJ and the adiabatic temperature reduced to 2303 K whereas the weight percentage of $MgAl_2O_4$ melt is reduced to zero and that of $MoSi_2$ is reduced to 65.

XRD patterns of the combustion products contain extra amounts of MgO (15 and 25 wt%) are given in Fig. 5. $MgAl_2O_4$ phase is still the main phase; Mo_5Si_3 phase has moderate intensity lines while both Si and $MoSi_2$ phases are vanished. The diffraction patterns of Mg_2SiO_4 and Mo are also detected. The extra amounts of MgO consume some amount of silica according to the side reaction:

$$2MgO + SiO_2 = Mg_2SiO_4 \qquad (9)$$

This leads to disappearance of both Si and $MoSi_2$ and appearance of Mo. Therefore lowering the combustion temperature by MgO additions does not give the anticipated action.

3.5. Effect of working pressure

Increasing the reaction pressure is expected to halt the volatilization of MoO_3 which is thought to corrupt the progress of reaction (4) to its completion. The pressure inside the combustion reactor is increased to 50 bar of argon.

XRD analysis of the combustion product at these conditions is given in Fig. 6 and compared with that of reaction under normal pressure. The intensity of the lines corresponding to Mo_5Si_3 and Si is highly minimized while the diffraction pattern of $MoSi_2$ phase increased to a high extent with the appearance of another $MoSi_2$ phase.

Furthermore, a trial is done at 1.0 atmospheric pressure of argon in order to synthesize the Mo_5Si_3 phase as reinforcement to $MgAl_2O_4$ matrix according to Eq. (5). Increasing the stoichiometric value of MoO_3 to that equivalent to the formation of Mo_5Si_3 gives rise to explosive reaction with blowing out of the entire product. This is due to the immense amount of liberated energy during this reaction (5) ($\Delta H = -5803$ kJ) which is about five times the heat liberated from reaction (4). The calculated adiabatic temperature was 3210 K. Therefore, the pressure inside the reaction chamber is increased to 50 bar argon and then ignition is carried out for the powder blend. XRD diagram of the combustion product, Fig. 7, shows only two diffraction patterns are indexed; the diffraction pattern of $MgAl_2O_4$ and the one correspond to the main phase Mo_5Si_3. No existence of any lines of $MoSi_2$ or free silicon.

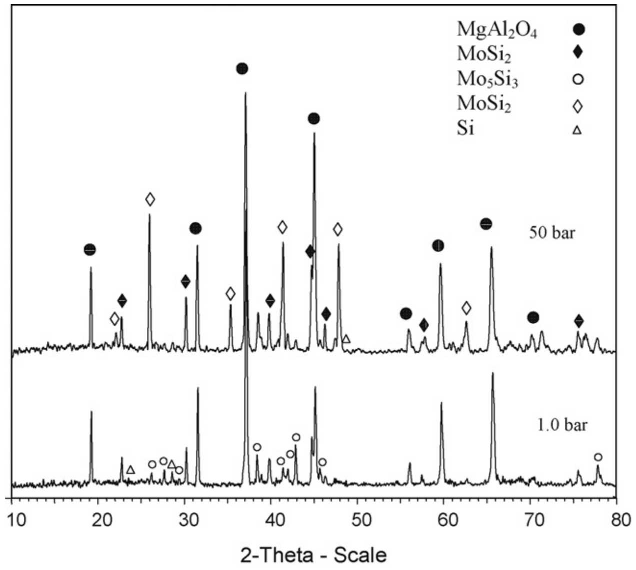

Fig. 6. Effect of reaction pressure on the completion of the formation reaction of $MoSi_2/MgAl_2O_4$.

3.6. Microscopic investigation

SEM images of the microstructure of the combustion products of $MoSi_2/MgAl_2O_4$ and $Mo_5Si_3/MgAl_2O_4$ composites prepared at 50 bar argon are given in Fig. 8. The microstructure of $MoSi_2/MgAl_2O_4$ shows agglomerations of the intermetallic phase in balls of different volumes impeded in the spinel matrix while that of $Mo_5Si_3/MgAl_2O_4$ composite shows complete agglomeration of Mo_5Si_3 phase in one ball in the middle of the sample which is completely separated from the ceramic part

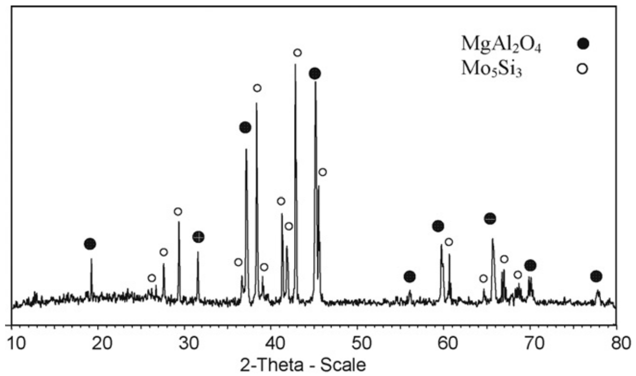

Fig. 7. Effect of reaction pressure on the completion of the formation reaction of $Mo_5Si_3/MgAl_2O_4$.

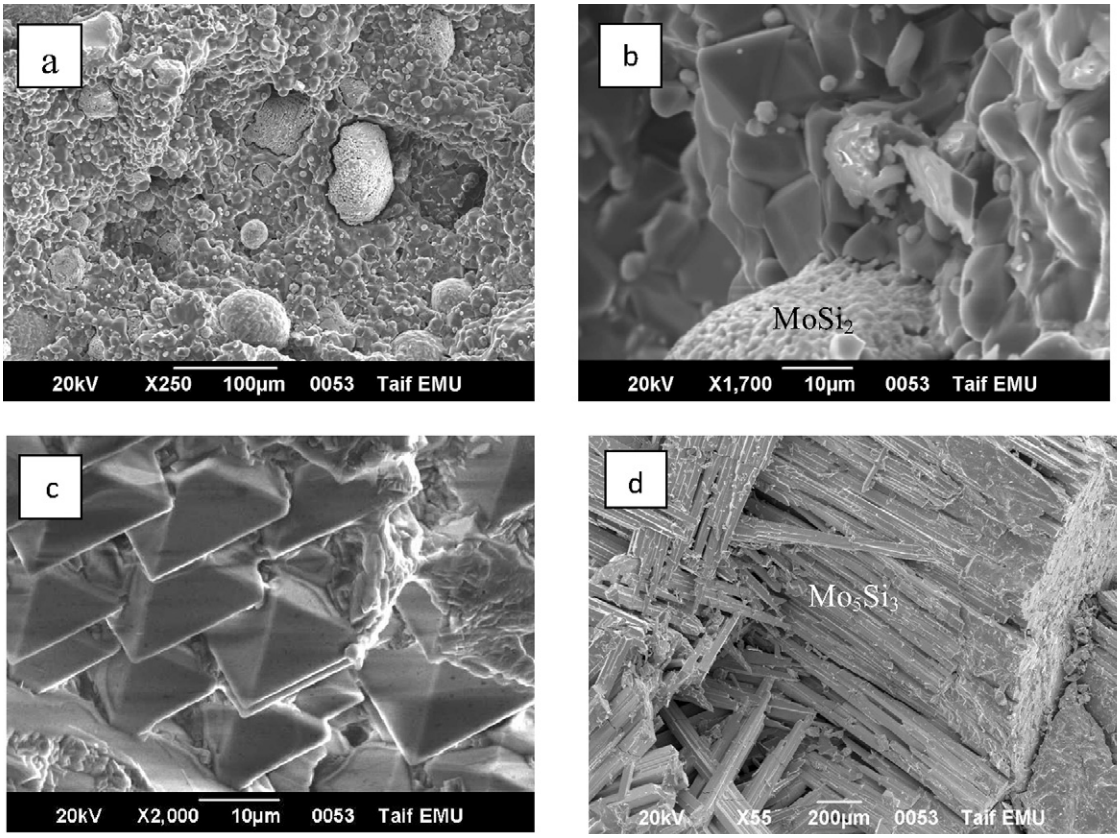

Fig. 8. SEM images: (a) and (b) are low and high magnifications of $MoSi_2/MgAl_2O_4$ composite; (c) and (d) are ceramic and intermetallic parts of $Mo_5Si_3/MgAl_2O_4$ composite.

$MgAl_2O_4$. This suggests that the combustion temperatures are higher than the melting points of the two silicide phases in the two composites which are in a good accordance with the thermodynamic study of these systems. Furthermore, the adiabatic temperature in case of $MoSi_2/MgAl_2O_4$ composite (T_{ad} = 2408 K) is close to the melting point of $MoSi_2$ (2303 K) while its value (T_{ad} = 3210 K) in case of $Mo_5Si_3/MgAl_2O_4$ is highly far from the melting point of Mo_5Si_3 (2465 K). This explains the agglomeration of silicides in several balls and in only one ball in case of $MoSi_2$ and Mo_5Si_3 respectively. The SEM micrographs of the ceramic part ($MgAl_2O_4$) show the formation of typical spinel structure with its identical pyramidal shapes.

4. Conclusion

$MgAl_2O_4/MoSi_2$ and $MgAl_2O_4/Mo_5Si_3$ composites have been successfully prepared by self-propagating high temperature synthesis method. Al powder of -5 μm grain size was important to avoid the formation of Al_2SiO_5. In case of $MgAl_2O_4/MoSi_2$ composite, working at 1.0 atm. of argon led to blowing out of some MoO_3 which contributed to the formation of Mo_5Si_3 phase and residual silicon in the product. While in case of $MgAl_2O_4/Mo_5Si_3$ composite the entire product was exploded and blown out. Increasing the pressure to 50 bar was found to suppress volatilization from the reaction media where both Mo_5Si_3 and free silicon were minimized in case of $MgAl_2O_4/MoSi_2$ and only $MgAl_2O_4$ and Mo_5Si_3 were formed in case of $MgAl_2O_4/Mo_5Si_3$ composite. It is worthy to mention although this work has succeeded in obtaining the target phases. However, the combustion products were highly porous (∼31 vol.%) and cracked in addition to lack of homogeneity between the obtained phases.

References

[1] H. Reveron, D.G. Campos, R.M. Rodriguez, J.C. Bonassin, Chemical synthesis and thermal evolution of $MgAl_2O_4$ spinel precursor prepared from industrial gibbsite and magnesia powder, Mater. Lett. 56 (1–2) (2002) 97–101.
[2] W.D. Kingery, D.R. Uhlmann, Introduction to Ceramics, Wiley, New York, 1976.
[3] A.F. Dericioglu, Y. Kagawa, Effect of grain boundary microcracking on the light transmittance of sintered transparent $MgAl_2O_4$, J. Eur. Ceram. Soc. 23 (6) (2003) 951–959.
[4] Y. Shimizu, H. Arai, T.S. Seiyama, Theoretical studies on the impedance-humidity characteristics of ceramic humidity sensors, Sensors Actuators 7 (1) (1985) 11–22.
[5] G. Gusmano, G. Montesperelli, E. Travera, A. Bearzotti, Humidity-sensitive electrical properties of $MgAl_2O_4$ thin-films, Sensors Actuators B 13–14 (1993) 525–527.
[6] L. Ji-Guang, T. Ikegami, L. Jong-Heun, T. Mori, Fabrication of translucent magnesium aluminum spinel ceramics, J. Am. Ceram. Soc. 83 (11) (2000) 2866–2868.

[7] B. Alinejad, H. Sarpoolaky, A. Beitollahi, A. Saberi, S. Afshar, Synthesis and characterization of nanocrystalline $MgAl_2O_4$ spinel via sucrose process, Mater. Res. Bull. 43 (2008) 1188–1194.

[8] V.T. Gritsyna, YuG. Kazarinov, V.A. Kobyakov, I.E. Reimanis, Radiation-induced luminescence in magnesium aluminate spinel crystals and ceramics, Nucl. Instrum. Methods Phys. Res. B 250 (1–2) (2006) 342–348.

[9] I. Ganesh, G.J. Reddy, G. Sundararajan, S.M. Olhero, P.M.C. Torres, J.M.F. Ferreira, Influence of processing route on microstructure and mechanical properties of $MgAl_2O_4$ spinel, Ceram. Int. 36 (2010) 473–482.

[10] J. Salmones, J.A. Galicia, J.A. Wang, M.A. Valenzuela, G. Aguilar-Rios, 1 Synthesis and characterization of nanocrystalline $MgAl_2O_4$ spinels as catalysts support, J. Mater. Sci. Lett. 19 (2000) 1033–1037.

[11] Z. Yao, J. Stiglich, T.S. Sudarshan, Molybdenum silicide based materials and their properties, J. Mater. Eng. Perform. 8 (3) (1999) 291–304.

[12] I. Tateoki, M. Toshihiro, Y. Hiroyuki, K. Hideki, Microstructure and properties of Mo_5Si_3-particle-reinforced Si_3N_4-matrix composites, J. Am. Ceram. Soc. 85 (4) (2002) 954–960.

[13] R.J. Bratton, Co precipitates yielding $MgAl_2O_4$ spinel powders, Am. Ceram. Soc. Bull. 48 (8) (1969) 759–762.

[14] P.W.D. Mitchell, Chemical method for preparing $MgAl_2O_4$ spinel, J. Am. Ceram. Soc. 55 (9) (1972) 484.

[15] J.G.M. DeLau, Preparation of ceramic powders from sulphate solutions by spray drying and roasting, Am. Ceram. Soc. Bull. 49 (6) (1970) 572–574.

[16] C.T. Wang, L.S. Lin, S.J. Yang, Preparation of $MgAl_2O_4$ spinel powders via freeze-drying of alkoxide precursors, J. Am. Ceram. Soc. 75 (8) (1992) 2240–2243.

[17] Y. Suyama, A. Kato, Characterization and sintering of Mg–Al spinel prepared by spray-pyrolysis technique, Ceram. Int. 8 (1) (1982) 17–21.

[18] A. Ghosh, R. Sarkar, B. Mukherjee, S.K. Das, Effect of spinel content on the properties of magnesia-spinel composite refractory J, Eur. Ceram. Soc. 24 (2004) 2079–2085.

[19] A.D. Mazzoni, M.A. Sainz, A. Caballero, E.F. Aglietti, Formation and sintering of spinels ($MgAl_2O_4$) in reducing atmospheres, Mater. Chem. Phys. 78 (2003) 30–37.

[20] H.C. Park, Y.B. Lee, K.D. Oh, F.L. Riley, Grain growth in sintered $MgAl_2O_4$ spinel, J. Mater. Sci. Lett. 16 (22) (1997) 1841–1844.

[21] Y.L. Jeng, E.J. Lavernia, Review: processing of molybdenum disilicide, J. Mater. Sci. 29 (1994) 2557–2571.

[22] N.S. Stoloff, An overview of powder processing of silicides and their composites, Mater. Sci. Eng. A 261 (1999) 169–180.

[23] S.C. Deevi, N.N. Thadhani, Reaction synthesis of high-temperature silicides, Mater. Sci. Eng. A 192/193 (1995) 604–611.

[24] P. Feng, X. Qu, F. Akhtar, S.H. Islam, Self-propagating high temperature synthesis of $MoSi_2$ matrix composites, Rare Metals 25 (3) (2006) 225–230.

[25] P. Mossino, Some aspects in self-propagating high temperature synthesis, Ceram. Int. 30 (2004) 311–332.

[26] C.R. Bowen, B. Derby, Self-propagating high temperature synthesis of ceramic materials, Br. Ceram. Trans. 96 (1) (1997) 25–31.

[27] A. Makino, C. Law, SHS combustion characteristics of several ceramics and intermetallic compounds, J. Am. Ceram. Soc. 77 (3) (1994) 778–786.

[28] P. Peralta, R. Dickerson, J.R. Michael, K.J. McClellan, F. Chu, T.E. Mitchell, Residual thermal stress in $MoSi_2$–Mo_5Si_5 in situ composites, Mater. Sci. Eng. A 261 (1–2) (1999) 261–269.

[29] J. Subrahmanyam, Combustion synthesis of $MoSi_2$–Mo_5Si_5, J. Mater. Res. 9 (10) (1994) 2620–2626.

[30] D.P. Mason, D.C. Van Aken, J.F. Mansfield, On the microstructure and crystallography of directionally solidified $MoSi_2$–Mo_5Si_5 eutectic, Acta Metall. Mater. 43 (3) (1995) 1189–1199.

[31] D.P. Mason, D.C. Van Aken, On the creep of directionally solidified $MoSi_2$–Mo_5Si_5 eutectic, Acta Metall. Mater. 43 (3) (1995) 1201–1210.